

Magnetic-Resonance Study of Iron in Silver Chloride*

JOHN CAMPBELL GARTH†

Department of Physics and Materials Research Laboratory, University of Illinois, Urbana, Illinois

(Received 25 January 1965)

The cubic electron-spin-resonance spectrum of Fe^{3+} in silver chloride has been studied at 1.3°K by the electron-nuclear-double-resonance (ENDOR) technique. ENDOR lines from 6 to 24 Mc/sec were observed on each of the five electron-spin-resonance transitions and have been identified as lines due to four chlorine nuclei which are nearest neighbors to the iron ion. The angular dependence of the crystal-field splitting of the electron resonance, as the orientation of the applied field is varied, proves that the iron is in a site of cubic symmetry. The angular variation of the ENDOR spectrum, as the field is rotated in a (100) plane, shows that the iron cannot be in a site of octahedral symmetry and that it therefore must be in a site of tetrahedral symmetry. ENDOR lines of both chlorine isotopes were identified. Cl^{35} ENDOR lines, characterized by $M_s = +\frac{3}{2}$ and $M_s = -\frac{3}{2}$, were studied with the applied field parallel to the [100] direction, and the best chlorine hyperfine and quadrupole coupling constants were determined for both isotopes. It is found that these constants can be used to predict the locations of all observed Cl^{35} and Cl^{37} ENDOR lines, but some discrepancies between the predicted spectrum and the observed lines remain which cannot be accounted for by effects of the cubic-field splitting term in the spin Hamiltonian.

I. INTRODUCTION

HENNING¹ and Hayes, Pilbrow, and Slifkin² have reported observation of an electron-spin-resonance spectrum of ferric iron ions in silver chloride. The spectrum possesses cubic symmetry and is attributed to iron located at an interstitial site² with four nearest-neighbor silver ions missing. They observed partially resolved superhyperfine structure on the central line of the five-line spectrum and attribute it to hyperfine interactions of the iron with the four nearest-neighbor chlorine ions arranged in a tetrahedron about the iron.

Determination of the model for this center is the central question with which we are concerned. The fact that a cubic spectrum for Fe^{3+} is observed at all is somewhat remarkable, because the two extra positive charges on the ferric ion should readily attract negative silver-ion vacancies. The presence of one or two vacancies nearby would destroy the cubic symmetry of the environment of the iron and give rise to a spectrum with lower symmetry.

At least four possible models for ferric iron in silver chloride yielding a cubic spectrum can be found. One is the substitutional model in which iron is substituted for a silver ion at a normal lattice position with no vacancies nearby. This site possesses octahedral symmetry and has six chlorine nearest neighbors along [100] directions from the iron site. The uncompensated charge of this center is $+2e$.

The other three models have tetrahedral symmetry. One is iron located at an interstitial site with four chlor-

ine and four silver nearest neighbors. The net charge of this center is $+3e$. Two tetrahedrons, one of silver ions and one of chlorine ions, surround the iron in such a way that, if the lattice were made up of point charges, the term $C(x^4+y^4+z^4-3r^4/5)$ of the electrostatic potential of the crystalline field would vanish, since the potential is odd under inversion. This potential (considered to be the term in the crystal field responsible for the cubic splitting term³ in the spin Hamiltonian) may therefore be expected to be small and to give rise to an extra small cubic field splitting. However, the fact that the observed cubic field-splitting parameter a is found to be as large as that for iron in typical octahedral and tetrahedral sites^{3,4} makes this model for the center appear to be less likely than the other three models.

Another more likely tetrahedral model is the model proposed by Hayes, Pilbrow, and Slifkin² which is iron in an interstitial site with four silver ions missing. This model, which has a net charge of $-e$, has been called² a "tetrahedral complex," since it resembles a FeCl_4^- molecular ion imbedded in the lattice. The creation of such a site does require association of the iron with four silver-ion vacancies, however.

Another molecular-ion model, which has the same tetrahedral symmetry, is that formed by substituting a FeCl_4^- complex for a Cl^- ion at a normal chlorine lattice position. Such a model has the objection that the FeCl_4^- complex would not fit easily into such a lattice position, but it has the attractive feature of having no net charge and hence requiring no vacancies to compensate its charge. We mention this model to show that it is possible to have a model with tetrahedral symmetry which is not centered on an interstitial site.

We report here the observation of chlorine electron-nuclear-double-resonance (ENDOR)⁵ lines observed

* Supported in part by the U. S. Atomic Energy Commission under Contract AT(11-1)-1198. The use of the IBM 7094 Computer was supported by the National Science Foundation.

† Present address: Department of Physics, Worcester Polytechnic Institute, Worcester, Massachusetts. This paper is based on a thesis submitted in partial fulfillment of the requirements for the degree of Doctor of Philosophy, Department of Physics, University of Illinois.

¹ K. Hennig, *Phys. Status Solidi* **3**, K458 (1953).

² W. Hayes, J. R. Pilbrow, and L. M. Slifkin, *J. Phys. Chem. Solids* **25**, 1417 (1964).

³ W. Low, *Paramagnetic Resonance in Solids* (Academic Press Inc., New York, 1960), p. 116.

⁴ S. Geschwind, *Phys. Rev.* **121**, 363 (1961); R. S. Title, *ibid.* **131**, 623 (1963).

⁵ G. Feher, *Phys. Rev.* **105**, 1122 (1957).

on all five spin-resonance transitions of the iron cubic spectrum at 1.3°K. The angular variation of the ENDOR spectrum indicates that the site is tetrahedral with four chlorine nearest neighbors aligned along [111] directions with respect to the iron. Further ENDOR experiments for more distant nuclei are required to distinguish between the three tetrahedral models cited above. Spin-Hamiltonian constants are obtained for the chlorine-35 isotope for both the $M_s = +\frac{3}{2}$ and the $M_s = -\frac{3}{2}$ spectrum, when the applied field is aligned along a [100] direction. The average hyperfine and quadrupole constants obtained for the Cl^{35} isotope are $A_s = 8.40 \pm 0.04$ Mc/sec, $A_p = 1.57 \pm 0.06$ Mc/sec, and $Q' = 5.74 \pm 0.09$ Mc/sec.

II. EXPERIMENTAL

Silver chloride samples used in this work were cut from boules grown from the melt by Kodak Research Laboratories.⁶ Spectrochemical analysis showed that the molar concentration of iron was about 6 ppm. After several steps of orientation and etching under red safe-light, rectangular samples, 16 mm × 9 mm × 2 mm, were cut with broad faces parallel to a (100) plane and edges parallel to <100> axes. The technique of epitaxial growth of KCl crystals onto the surface of a boule⁷ was used for a preliminary orientation of samples, and the final orientation was made by x-ray back reflection. The etching treatment of the samples before heat treatment in a chlorine atmosphere was similar to that described by Sliker.⁸

For heating, the freshly etched sample was placed on a quartz plate and inserted into a Pyrex tube, blackened with Aquadag to prevent light from entering the tube. The tube was attached to a vacuum system and a furnace placed around the tube. The sample was gradually heated in vacuum to about 300°C in 8 h. The slow warm-up was found necessary to anneal remaining strain in the samples; raising the temperature to 300°C in about an hour occasionally resulted in samples turning polycrystalline. Chlorine was distilled and added to the tube to a pressure of 1 atm. The temperature of the furnace was raised to 385°C and kept at this temperature for 8 to 12 h.

After heating, the furnace was quickly withdrawn from the sample tube, and the tube was cooled to room temperature with a blower in less than 5 min. Chlorine was then removed from the tube, air admitted, and the sample tube removed from the vacuum system.

The sample was placed flat against the side wall of the microwave cavity, and the cavity was packed tightly with styrofoam to hold the sample securely and to prevent microphonic noise. The two halves of the

cavity, split along a microwave current nodal plane, were insulated with a 5-mil-thick Mylar strip in order to permit introduction of the ENDOR rf field by currents induced on the inside wall of the cavity by a five-turn ENDOR coil.⁹ The cavity was wrapped with glass tape, wound with the ENDOR coil, mounted onto a waveguide cavity mount and plunged into liquid nitrogen to quench the silver chloride within a half-hour after halogenation.

Electron-spin-resonance (ESR) and ENDOR runs were performed on a superheterodyne X-band spectrometer, built originally by Holton and Blum⁹ and modified to lock the klystron onto the sample cavity frequency.¹⁰ Runs were made at 1.3°K with the cavity immersed in a bath of liquid helium pumped on by a high-capacity vacuum pump. The power to the ENDOR coil was supplied from a high-power rf oscillator¹¹ square-wave amplitude modulated at 320 cps and swept in frequency by means of a motor-driven gear drive rotating the tuning condenser of the oscillator. The ENDOR frequency was read from a Hewlett-Packard Model 524C cycle counter, and frequency markers were placed manually at 50 kc/sec intervals on the chart recording.

ENDOR lines were observed with maximum signal-to-noise ratio when the microwave power to the cavity was set to about 45 dB below the 500-mW output of the V-58 klystron. ENDOR power of about 1 W was delivered to the coil around the cavity, raising the temperature of the helium bath to about 1.7°K. The ENDOR lines were observed on each of the five ESR transitions with the magnetic field set near to the absorption peak (zero first derivative) of each transition.

The range of the ENDOR oscillator was from 0.8 to 24 Mc/sec, obtained by changing coils. A large number of closely spaced ENDOR peaks were seen between 1 and 3 Mc/sec in the region of the "distant ENDOR"¹² frequencies for the two chlorine isotopes. Very few lines on any ESR transition were seen between 3 and 6 Mc/sec. The ENDOR lines discussed in this paper were those in the range from 6 to 24 Mc/sec.

Using two different samples, three sets of ENDOR data were taken. The conditions for the three sets of data were the following:

(1) With a poorly aligned sample, ENDOR frequency spectra were recorded for each of the five ESR transitions with the external field fixed at an angle of 10 deg with respect to a [100] direction.

(2) With a better aligned sample (and a slightly lower microwave cavity frequency), ENDOR frequency spectra were recorded for each of the five ESR transi-

⁹ W. C. Holton and H. Blum, *Phys. Rev.* **125**, 89 (1962); W. C. Holton, thesis (unpublished), University of Illinois, 1961.

¹⁰ The spectrometer was modified to lock the klystron onto the sample cavity by J. C. Bushnell.

¹¹ The ENDOR oscillator was designed and constructed by J. H. Pifer and C. H. Henry.

¹² J. Lambe, N. Laurance, E. C. McIrvine, and R. W. Terhune, *Phys. Rev.* **122**, 1161 (1961).

⁶ Samples were obtained through the courtesy of Professor F. C. Brown.

⁷ Growth of epitaxial crystals for orientation of silver chloride boules was suggested by Dr. D. W. Burnham of Kodak Research Laboratories.

⁸ T. R. Sliker, *Phys. Rev.* **130**, 1749 (1963).

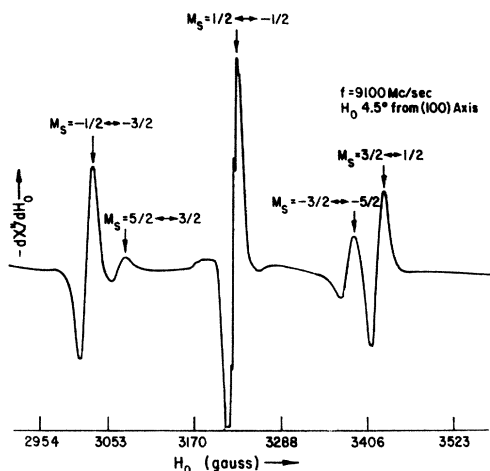


FIG. 1. Cubic electron-spin-resonance spectrum of Fe^{3+} in silver chloride at 1.3°K .

tions with the external field at an angle of 0.5 deg from a $[100]$ direction.

(3) Using the same sample as in (2), the angular dependence of the ENDOR spectrum observed on the $M_s = +\frac{3}{2} \leftrightarrow M_s = +\frac{1}{2}$ ESR transition was studied with the external field rotated from a $[100]$ direction to a $[110]$ direction in a (100) plane.

III. ELECTRON-SPIN-RESONANCE SPECTRUM

Figure 1 shows the cubic spectrum of iron in silver chloride at 1.3°K with the external field nearly parallel to a $[100]$ direction (4.5 deg from a $[100]$ direction). The five lines of the spectrum are the five $\Delta M_s = \pm 1$ transitions for the six spin states of a Fe^{3+} ion (${}^6S_{5/2}$) with a strong Zeeman interaction and a relatively weak cubic-field interaction. (M_s is the eigenvalue of the component of S along the external field.) These interactions may be described by the spin Hamiltonian

$$\mathcal{H}_{\text{el}} = g\beta\mathbf{H}_0 \cdot \mathbf{S} + (a/6)[S_x^4 + S_y^4 + S_z^4 - S(S+1)(3S^2 + 3S - 1)] \quad (1)$$

which describes the spectrum and its angular variation with $g = 2.018 \pm 0.002$ and $a = (+76 \pm 4) \times 10^{-4} \text{ cm}^{-1}$.

The identification of the two quantum numbers M_s for each of the five spin-resonance transitions is easily obtained at this low temperature and is necessary for analysis of the ENDOR spectrum. The Boltzmann factor, $\exp(g\beta H_0/kT)$, giving the ratio of populations of adjacent M_s levels, is appreciably greater than one at $T = 1.3^\circ\text{K}$. Therefore, the more negative M_s levels, having lower energy, are more heavily populated than the positive M_s levels, and consequently the negative M_s spin transitions are more intense than the corresponding positive M_s transitions. The identification shown in Fig. 1 follows from the known relative positions of the lines of the cubic spectrum and the observed

relative intensities. This method of identification establishes the usual result that the sign of a is positive.¹³

The central line of the spectrum, the $M_s = \frac{1}{2} \leftrightarrow -\frac{1}{2}$ transition, exhibits superhyperfine structure when the external field is parallel to either a $[100]$ or a $[111]$ direction.^{1,2} Figure 2 shows the peculiar pattern observed at 1.3°K when the external field is parallel to a $[100]$ direction; the structure is incompletely resolved and is not symmetric about the center of the resonance. There appear to be at least 20 partially resolved superhyperfine structure components. As the ENDOR results to be presented confirm, these lines must be attributed to four equivalent, tetrahedrally located, chlorine ions aligned along $[111]$ directions with respect to the iron. (By approximate fitting of the superhyperfine structure pattern observed at 20°K , Hayes, Pilbrow, and Slifkin² have shown that the structure, in order to be explained, must be described by a large quadrupole interaction as well as an axially symmetric hyperfine interaction.)

The complete spin Hamiltonian for iron in a cubic site, interacting with n -equivalent neighboring chlorine nuclei, is

$$\mathcal{H} = \mathcal{H}_{\text{el}} + \sum_{i=1}^n \{ -\gamma_n \hbar \mathbf{H}_0 \cdot \mathbf{I}_i + A I_{iz_i} S_{zi} + B(I_{xz_i} S_{xz_i} + I_{iy_i} S_{iy_i}) + Q'[I_{zz_i}^2 - \frac{1}{3}I(I+1)] \}. \quad (2)$$

This spin Hamiltonian may be used to describe either a tetrahedral or an octahedral site. For these two cases, the summation is over $n = 4$ or 6 , respectively. Because of either the three- or fourfold symmetry of the chlorine-iron axes, the hyperfine interaction may be assumed to be axially symmetric and is written in Eq. (2) in the form $A I_x S_x + B I_y S_y$. We shall henceforth use the equivalent form $A_s \mathbf{I} \cdot \mathbf{S} + A_p(3I_z S_z - \mathbf{I} \cdot \mathbf{S})$, where A_s and A_p are the isotropic and anisotropic hyperfine interaction parameters, $A_s = (A + 2B)/3$, and $A_p = A - B$.

As the microwave power to the cavity is increased, the electron-spin-resonance spectrum signal saturates

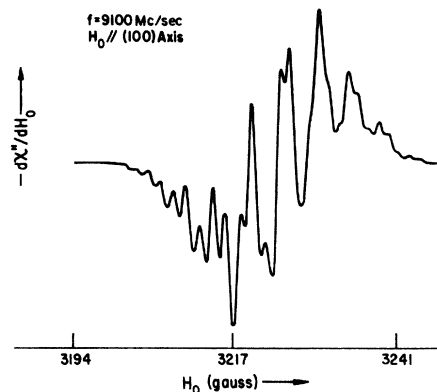


FIG. 2. $M_s = +\frac{1}{2} \leftrightarrow -\frac{1}{2}$ transition at 1.3°K showing superhyperfine structure of chlorine nuclei.

¹³ W. Low, Phys. Rev. **105**, 792 (1957).

at a power level as low as 50 dB below 500 mW. The maximum ENDOR signal heights were observed at 45 dB below 500 mW. No saturation of the resonance signal was observed at liquid-nitrogen temperature.

A study was made of the effect of different rates of cooling on the cubic spectrum observed at liquid-nitrogen temperature. (Similar studies made on Cu^{++} in AgCl by Tucker¹⁴ enabled him to vary the relative numbers of unassociated Cu^{++} ions and ions associated with vacancies.) The following effects of different rates of cooling on the spectrum observed at 77°K were noted:

(1) Cooling the sample rapidly from 385°K to room temperature (in about five minutes) and subsequent quenching of the sample in liquid nitrogen gave the maximum signal strength of the cubic spectrum with no other resonance lines observed.

(2) Cooling the sample gradually in chlorine from 385°C to room temperature in about two hours and quenching the sample in liquid nitrogen caused the cubic spectrum to disappear completely. Instead, resonances at $g=2$ about 500-G broad were observed.

(3) Cooling the sample in 5 min to room temperature, quenching in liquid nitrogen, warming to room temperature, and cooling the sample gradually for 8 h to liquid nitrogen yielded a cubic spectrum of about one-third the size obtained by quenching in liquid nitrogen.

(4) Warming the sample treated as in (3) to room temperature and then quenching in liquid nitrogen restored the signal to about two-thirds of the signal height seen in the "freshly quenched" sample.

(5) Cooling the sample rapidly from 385°C to room temperature, leaving the sample at room temperature for 6 to 24 h, and quenching the sample in liquid nitrogen yielded a greatly decreased cubic spectrum signal.

(6) A silver chloride crystal doped with 700 ppm iron¹⁵ was halogenated and cooled rapidly in the same manner as the 6-ppm samples, but no electron-spin-resonance signals were detected. The boules, grown in a very dilute chlorine atmosphere and annealed slowly for 30 h, were initially transparent and pale yellow. After heat treatment in either a chlorine atmosphere or in vacuum, samples turned a deep orange, probably indicating precipitation of FeCl_3 . Similar behavior for samples heavily doped with iron by diffusion has been reported by Sliker.¹⁶

From these studies, it is apparent that the cubic iron centers created at a high temperature are destroyed by annealing at moderate temperatures both above and below room temperature. The centers are stable at liquid-nitrogen temperature (samples stored for 3 months at liquid-nitrogen temperature retained their original signal strength). The role of vacancy association

in destroying these centers is not clear from these experiments. It seems likely that the iron coagulates readily into a precipitated phase which yields either a very broad resonance or no observable resonance signal.

IV. ENDOR RESULTS: ANGULAR-VARIATION STUDIES

A. Symmetry Considerations

It is the angular variation of the ENDOR spectrum which establishes the symmetry of the site as tetrahedral rather than octahedral. In order to discuss the variation of the ENDOR frequencies as the external field is rotated in a (100) plane, we first state the symmetry arguments used to interpret these results.

Our starting point is the spin Hamiltonian of Eq. (2). The part of the Hamiltonian which contains the nuclear spin coordinates of one nucleus may be called the nuclear Hamiltonian. The nuclear Hamiltonian for each chlorine nucleus in Eq. (2) can be written as

$$\mathcal{H}_{\text{nuc1}} = A_s \mathbf{I} \cdot \mathbf{S} + A_p (3I_z S_z - \mathbf{I} \cdot \mathbf{S}) + Q' [I_z^2 - I(I+1)/3] - \gamma_n \hbar \mathbf{H}_0 \cdot \mathbf{I}. \quad (3)$$

This Hamiltonian reflects the cubic symmetry of the iron site. The z axis is the iron-chlorine axis. If the site is octahedral, the z axis is a $\langle 100 \rangle$ axis and has fourfold symmetry, while, if the site is tetrahedral, the z axis is a $[111]$ axis and has threefold symmetry. In either case, the hyperfine interaction is axially symmetric and includes only two independent hyperfine constants. Since the quadrupole axis is the same as the hyperfine symmetry axis, the quadrupole interaction is axially symmetric and the asymmetry parameter of the quadrupole interaction is zero.

We may solve the nuclear-spin-energy eigenvalue problem for the Hamiltonian in Eq. (3), if we integrate over the electron spin coordinates keeping only terms diagonal in the electron spin component along the external field direction. This procedure, which may be called the "effective-field" approximation,^{17,18} enables us to lump together the magnetic interactions of the nuclear spin with both the electron spin (the hyperfine interaction) and the external field into one Zeeman interaction with an effective magnetic field \mathbf{H}_{eff} . In this approximation, Eq. (3) may be rewritten

$$\mathcal{H}_{\text{nuc1}}(\text{effective}) = -\gamma_n \hbar \mathbf{H}_{\text{eff}} \cdot \mathbf{I} + Q' [I_z^2 - I(I+1)/3]. \quad (4)$$

This Hamiltonian is a true spin Hamiltonian since it involves only the nuclear spin coordinates. It is the well-known Hamiltonian of a nucleus with a Zeeman and a quadrupole interaction. Since $I = \frac{3}{2}$ for each chlorine isotope, there are four nuclear-spin eigenstates. The

¹⁴ R. F. Tucker, Phys. Rev. **112**, 725 (1958).

¹⁵ Grown by Dr. Scott Anderson of the Anderson Physical Laboratory.

¹⁶ T. R. Sliker, thesis, Cornell University, 1962 (unpublished).

¹⁷ N. Laurance, E. C. McIrvine, and J. Lambe, J. Phys. Chem. Solids **23**, 515 (1962).

¹⁸ J. M. Baker and J. P. Hurrell, Proc. Phys. Soc. **82**, 742 (1963).

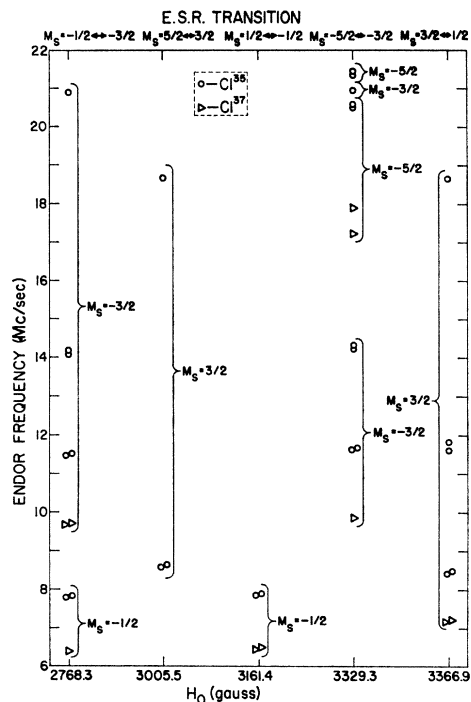


FIG. 3. ENDOR spectrum at 1.3°K with H_0 0.5 deg from a (100) axis.

solutions of the eigenvalue problem for this Hamiltonian have been tabulated.¹⁹

One other assumption which we must make is that the four chlorine energy levels are nondegenerate and do not "cross" as the external field is rotated with respect to each iron-chlorine symmetry axis (the z axis). The ENDOR frequencies are given by differences between the four energy levels of a chlorine spin. Subject to the effective field approximation, we can now deduce the angular-variation behavior of the ENDOR frequencies from the symmetry properties of the Hamiltonian given by Eq. (3).

As the external field is rotated with respect to the sample, it rotates with respect to the symmetry axes of the chlorine sites. If, as the field is rotated, the angle between it and a given chlorine z axis changes, the energy levels of the spin Hamiltonian of Eq. (4) derived from (3) change; if the angle does not vary as the field is rotated, the energy levels stay constant, because $\mathcal{H}_{\text{nucl}}$ is invariant to rotations of the external field about the axis of symmetry.

$\mathcal{H}_{\text{nucl}}$ is also invariant to reversal of the external field or to reflection of the field through the plane of symmetry perpendicular to the symmetry axis. This allows us to state that as we rotate the field through a direction perpendicular to the symmetry axis, the chlorine energy levels go through either maxima or minima.

¹⁹ P. M. Parker, J. Chem. Phys. 24, 1096 (1956); R. M. Steffen, E. Matthias, and W. Schneider, AEC Report TID-15749 (available from Office of Technical Services, Department of Commerce, Washington, D. C. for \$4.50).

The following statements about the angular behavior of the nuclear energy levels hold and also apply to ENDOR frequencies, since they are given by energy-level differences:

(1) As the external magnetic field is rotated in a plane containing a chlorine-iron symmetry axis, the four energy eigenvalues for that nucleus go through extrema (maxima or minima) when the field is (a) parallel to, or (b) perpendicular to the axis of symmetry.

(2) As the magnetic field is rotated in the plane perpendicular to a symmetry axis, the energy eigenvalues remain fixed, since $\mathcal{H}_{\text{nucl}}$ remains unchanged by such a rotation.

(3) As the field is rotated in a plane making an angle between 0 and 90 deg with the symmetry axis, the energy eigenvalues will have extrema (a) when the field is parallel to the projection of the symmetry axis onto the plane of rotation or (b) when the field is perpendicular to the symmetry axis.

The important corollary of these statements is that, if the energy levels for a given nucleus do *not* reach a maximum or a minimum when the field is parallel or perpendicular to a given axis, that axis *cannot* be the symmetry axis of that nucleus. The converse is not necessarily true, since it is conceivable that there are other directions in the plane of rotation of the field, besides those directions associated with the symmetry axis, in which the energy levels reach extrema.

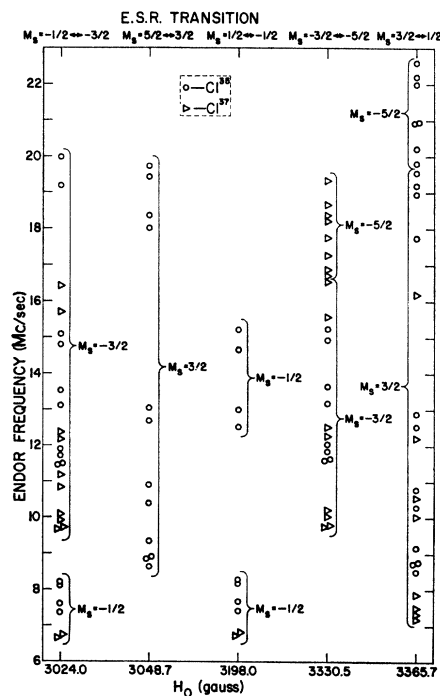


FIG. 4. ENDOR spectrum at 1.3°K with H_0 10 deg from a (100) axis.

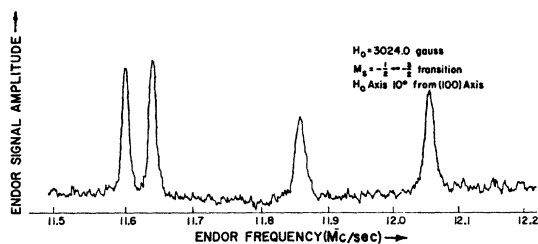


FIG. 5. Experimental ENDOR lines of large signal strength observed on the $M_s = -\frac{1}{2} \leftrightarrow -\frac{3}{2}$ transition for H_0 10 deg from a $\langle 100 \rangle$ axis.

The ENDOR frequencies produced by a given nucleus must reach extrema when the energy levels of that nucleus reach extrema. Therefore we have a criterion for deciding which crystalline axes are not and which probably are iron-chlorine symmetry axes from a study of the angular variation of the ENDOR spectrum. In particular, we look to see what directions in a $\langle 100 \rangle$ plane yield extrema of the ENDOR lines and which do not. Those directions in which *any* ENDOR spectra for a given nucleus do *not* reach extrema must be ruled out as possible symmetry axes of that nucleus. On the other hand, directions in which all the spectra for a given nucleus reach extrema *may* be symmetry axes.

B. Observed ENDOR Spectrum and Its Angular Variation

Figures 3 and 4 show the frequencies of ENDOR lines observed on each of the five electron-spin-resonance transitions, with the external field making fixed angles of 0.5 and 10 deg, respectively, with $\langle 100 \rangle$ axes of two different silver chloride samples. The frequencies are shown as points along five vertical scales corresponding to the five transitions. Each scale is labeled by the M_s and $M_s - 1$ values of the electron spin levels involved in each transition and by the magnetic field at the center of each transition.

An example of the experimental ENDOR data which have been plotted in Fig. 4 is shown in Fig. 5. The four peaks shown were observed on the $M_s = -\frac{1}{2} \leftrightarrow -\frac{3}{2}$ transition and were the largest ENDOR peaks observed on any of the five transitions. They represent "equivalent" ENDOR transitions of the four near-neighbor Cl^{35} nuclei of the tetrahedral site. These ENDOR peaks nearly coincide at 11.5 Mc/sec when the external field is 0.5 deg from a $\langle 100 \rangle$ axis, as is shown on the plot in Fig. 3. The same angular behavior is observed for all ENDOR frequencies shown in Figs. 3 and 4. Thus, Fig. 3 shows a spectrum having single lines or closely spaced pairs of lines, while Fig. 4 shows that these lines break up into groups of four lines centered approximately at the original positions shown in Fig. 3.

This angular behavior is readily explained by the tetrahedral site model. When the field is aligned along a $\langle 100 \rangle$ axis, the four z axes of the four tetrahedral chlo-

rine ions make the same angle with the field, while they make different angles with the field when it is not parallel to a $\langle 100 \rangle$ axis. In the first case, the nuclei yield the same set of ENDOR frequencies, while in the second case, the nuclear energy levels are no longer identical and give rise to different ENDOR frequencies.

Figure 6 shows the angular dependence of the ENDOR frequencies observed on the $M_s = +\frac{3}{2} \leftrightarrow \frac{1}{2}$ transition as the magnetic field is rotated in a $\langle 100 \rangle$ plane. (To perform this experiment, it was necessary to adjust the field so as to remain on the center of the transition as the field is rotated. This is because the positions of all transitions except the $M_s = +\frac{1}{2} \leftrightarrow -\frac{1}{2}$ transition vary with angle as the field is rotated.¹) In this figure, we see that all ENDOR frequencies reach maxima or minima when the field is approximately parallel to a $[110]$ direction (approximately, because the sample is not perfectly aligned), while some lines cross over each other and clearly *do not reach extrema* when the field is parallel to the $[100]$ direction. This may be taken as clear evidence that the site is not octahedral and therefore must be tetrahedral.

The observations that (1) all observed lines shown in Fig. 6 reach extrema when the field is parallel to a $[110]$ direction and (2) that lines which coincide when the field is parallel to a $[100]$ direction break into sets of four lines when the field is not parallel to a $[100]$ direction support the conclusion that the site is tetrahedral. The most direct evidence, however, is the fact that some of the ENDOR lines do not reach extrema when the field is parallel to a $[100]$ direction. If the tetrahedral and octahedral models described earlier are the only possible models for iron in a site of cubic symmetry, we have shown that the octahedral model cannot be correct and therefore that only a tetrahedral model can exhibit the angular dependence of the chlorine ENDOR lines shown in Fig. 6.

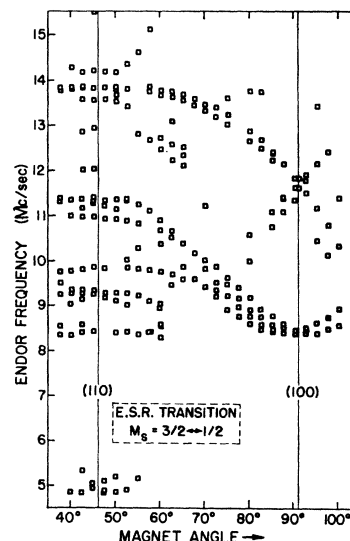


FIG. 6. Angular variation of ENDOR lines on the $M_s = +\frac{3}{2} \leftrightarrow +\frac{1}{2}$ transition as the field is rotated in a $\langle 100 \rangle$ plane.

V. ANALYSIS OF THE [100] ENDOR SPECTRUM

A. M_s Values of ENDOR Lines

Let us call the external field direction the z' axis. When the external field is parallel to a [100] direction, to an excellent approximation, the eigenvalue M_s of the electron spin component $S_{z'}$ along the z' axis is a good quantum number. Both the Zeeman and the cubic field interactions, except for a term $a(S_+^4 + S_-^4)/48$, are diagonal in $S_{z'}$; and this nondiagonal term produces only very slight mixing between the $M_s = +\frac{3}{2}$ and the $M_s = -\frac{5}{2}$ states, and between the $M_s = -\frac{3}{2}$ and the $M_s = +\frac{5}{2}$ states. Therefore, each electron spin level may be labeled by M_s and, furthermore, the expectation value of $S_{z'}$ for each M_s level is very nearly equal to M_s .

ENDOR transitions may be thought of as transitions between nuclear sublevels of one electron M_s level. In other words, when a nucleus is flipped, the electron spin stays fixed, since the electron-nuclear coupling is assumed to be much smaller than the electron Zeeman and cubic field interactions. Each ENDOR line may therefore be characterized by one value of M_s . Consequently, we can expect to see two sets of ENDOR lines on each electron-spin-resonance transition, $M_s \leftrightarrow M_s - 1$; one set will be characterized by M_s and the other by $M_s - 1$.

The ENDOR data shown in Figs. 3 and 4 are labeled by their M_s values. A positive identification of M_s values was made as follows: If the signal-to-noise ratio was large enough, lines of given M_s were observed on both the $M_s + 1 \leftrightarrow M_s$ and the $M_s \leftrightarrow M_s - 1$ electron-spin-resonance transitions. If the external field had not been changed in going from one transition to the other, the same ENDOR line would have had the same rf frequency on the two transitions. (This is because no parameter of the Hamiltonian describing the nuclear energy levels would have been changed.) However, the effect of changing the external field in going from one spin-resonance transition to the other was to change slightly both the magnitude and the direction of the total "effective" field seen by the nucleus. Therefore, ENDOR frequencies were shifted by an amount dependent on the change in field.

In Figs. 3 and 4, examples of corresponding ENDOR lines with the same M_s values, but with frequency shifts in the order of 100 kc/sec are:

- (1) for the two transitions involving $M_s = +\frac{3}{2}$, the ENDOR lines near 8.7 and 18.7 Mc/sec,
- (2) for $M_s = -\frac{3}{2}$, lines near 9.7, 11.5, 14.1, and 20.9 Mc/sec, and
- (3) for $M_s = -\frac{1}{2}$, lines near 7.8 and 6.5 Mc/sec.

This method of identification does not apply to $M_s = +\frac{5}{2}$ and $-\frac{5}{2}$ lines since they should occur on only one electronic transition. No $M_s = +\frac{1}{2}$ lines were found.

After spin-Hamiltonian parameters for both chlorine isotopes were obtained and the entire spectrum was

calculated, the M_s values of all the remaining ENDOR lines in Figs. 3 and 4 were assigned. In Fig. 3, lines near 18 and 21 Mc/sec were assigned to $M_s = -\frac{5}{2}$; the fact that these lines were seen only on the $M_s = -\frac{3}{2} \leftrightarrow -\frac{5}{2}$ transition supports this assignment. Similar lines are shown in Fig. 4, with the apparent irregularity that some $M_s = -\frac{5}{2}$ lines were seen with the field set on the $M_s = +\frac{3}{2} \leftrightarrow +\frac{1}{2}$ transition instead of the $M_s = -\frac{3}{2} \leftrightarrow -\frac{5}{2}$ transition. The explanation for this is not clear, but, since the two adjacent transitions were broad and not well resolved when the field was oriented 10 deg with respect to the (100) axis, it is likely that ENDOR lines from both transitions were seen at the same field setting.

B. Identification of Cl^{35} and Cl^{37} Lines

From the magnitude of the "field shifts" of the ENDOR lines, it was found that all the ENDOR lines from 6 to 24 Mc/sec were due to chlorine (see Appendix I). The great majority of the lines shown in Figs. 3 and 4 are Cl^{35} isotope lines. This is because the Cl^{35} is about 75% abundant and three times more abundant than the Cl^{37} isotope, and the signal-to-noise ratio is three times greater.

The most intense lines of the entire ENDOR spectrum are the four Cl^{35} lines shown in Fig. 5, taken with the field 10 deg from a (100) axis. The four corresponding Cl^{37} lines occur near 9.7 Mc/sec (plotted in Fig. 4) and were easily identified by their similar linewidth and similar relative spacing; their intensity was about a third the intensity of the Cl^{35} lines. Furthermore the ratio of the Cl^{35} frequency to the Cl^{37} frequency is about $11.5/9.7 = 1.185$, while the corresponding magnetic moment and quadrupole moment ratios are 1.20 and 1.27, respectively. The approximate agreement of the frequency ratio with the two nuclear moment ratios supports the isotope identifications of these ENDOR lines.

The other Cl^{37} lines plotted in Figs. 3 and 4 were identified in the same manner by their frequency and intensity ratios to Cl^{35} lines. In Fig. 4, sets of four Cl^{37} lines have similar relative spacings to their Cl^{35} counterparts. The positions of the Cl^{37} lines in Fig. 3 were confirmed by calculation of the spectrum from the Cl^{37} spin-Hamiltonian constants obtained from the Cl^{35} spin-Hamiltonian constants. Approximately correct prediction of the positions of Cl^{37} lines is taken as strong evidence that the magnitudes of the calculated Cl^{35} and Cl^{37} spin-Hamiltonian constants are approximately correct.

C. Spin-Hamiltonian Constants

Out of the six possible M_s values, only values equal to $+\frac{3}{2}$, $-\frac{1}{2}$, $-\frac{3}{2}$, and $-\frac{5}{2}$ were found for ENDOR lines. In Fig. 3, there are, for the Cl^{35} isotope, three distinct sets of lines for $M_s = +\frac{3}{2}$ and $M_s = -\frac{3}{2}$, two distinct sets of lines for $M_s = -\frac{5}{2}$, and one set for $M_s = -\frac{1}{2}$. The question now becomes: How can the Cl^{35} spin-

Hamiltonian constants, A_s , A_p , and Q' be calculated from these lines?

The spin of a chlorine nucleus of either isotope is $\frac{3}{2}$. If the energy levels for a chlorine nucleus is described by a spin Hamiltonian given by Eq. (4), where H_{eff} is a function of H_0 , A_s , A_p , M_s and the angle between the H_0 axis and the $\langle 111 \rangle$ axis, there are four distinct energy levels of the chlorine nuclear spin. A scheme showing the nuclear spin levels and possible ENDOR frequencies is shown in Fig. 7. There are six possible frequencies, ν_1 through ν_6 , which are defined in terms of the energy levels, as shown in Fig. 7, by $\nu_1 = E_2 - E_1$, $\nu_2 = E_3 - E_2$, etc., where E_1 , E_2 , E_3 , and E_4 are the energy levels in order of increasing energy.

There are six possible ENDOR frequencies for each nucleus for a given M_s value, but in Fig. 3, at most three ENDOR frequencies are observed. (The four chlorine nuclei of the tetrahedral site give rise to the same ENDOR frequencies when H_0 is parallel to a $\langle 100 \rangle$ axis.) We have no way of knowing *a priori* which of these six transitions we observe. (Even if we happened to know the eigenfunctions and the eigenvalues of the nuclear spin Hamiltonian, we would not be able to calculate the relative intensities of the six possible ENDOR transitions, since the cross-relaxation times and other details of the ENDOR mechanism are not yet known.)

Fortunately, if we are given frequencies of three independent ENDOR transitions (such that the sum of two is not equal to the third), and if we define the sum of the energy levels to be some value such as zero, we have enough information to find the four energy levels. (We assume the frequencies are positive in order to obtain the order of the energy levels as shown in Fig. 7.) Using sum rules for the energy levels of a spin- $\frac{3}{2}$ nucleus with a Zeeman and a quadrupole interaction,²⁰ we can then calculate several possible values for the spin-Hamiltonian constants. The method of calculating the spin-Hamiltonian constants is described in Appendix II.

The only M_s values for which we have three distinct ENDOR frequencies (neglecting the spacing between closely separated pairs of lines in Fig. 3) are $M_s = +\frac{3}{2}$ and $M_s = -\frac{3}{2}$ for the Cl^{35} isotope. Therefore, we can look for the solution of the spin-Hamiltonian constants from *only* either of these two sets of three frequencies. We can use the other observed frequencies as checks on the derived spin-Hamiltonian constants, but we cannot use them to derive the constants. (We therefore

TABLE I. $M_s = +\frac{3}{2}$ and $M_s = -\frac{3}{2}$ Cl^{35} ENDOR frequencies.

M_s	H_0 (G)	ν_x (Mc/sec)	ν_y (Mc/sec)	ν_z (Mc/sec)
$+\frac{3}{2}$	3366.9	11.655 ± 0.020	8.435 ± 0.010	18.6875 ± 0.020
$-\frac{3}{2}$	2968.3	14.1275 ± 0.020	11.4925 ± 0.020	20.890 ± 0.040

²⁰ L. C. Brown and P. M. Parker, Phys. Rev. **100**, 1764 (1955).

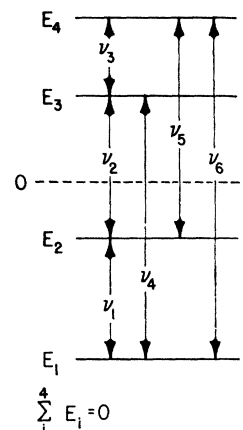


FIG. 7. Schematic energy-level diagram for a chlorine nuclear spin showing possible ENDOR transitions.

cannot calculate the Cl^{37} constants from Cl^{37} ENDOR frequencies, but can only assume that they may be obtained from the Cl^{35} constants by multiplying by the appropriate nuclear and quadrupole moment ratios.)

Table I lists the average values of the ENDOR frequencies observed for $M_s = +\frac{3}{2}$ and $M_s = -\frac{3}{2}$ for the Cl^{35} isotope, with H_0 0.5 deg from a $\langle 100 \rangle$ axis. We denote the three unknown transitions to which these frequencies correspond by ν_x , ν_y , and ν_z .

We now assume that these average frequencies correspond to the "exact" frequencies that would be seen if the magnetic field were perfectly aligned along a $[100]$ direction.

We have calculated the energy levels for every possible choice of ν_x , ν_y , and ν_z . For example, if we set $\nu_x = \nu_1$, $\nu_y = \nu_3$, and $\nu_z = \nu_4$, we can calculate ν_2 , ν_5 , and ν_6 as well as E_1 , E_2 , E_3 , and E_4 . Using sum rules involving ν_1 , ν_2 , and ν_3 , we have then calculated all possible quadrupole and hyperfine constants, Q' , A_s , and A_p , and listed them in Table II. Since it usually turns out that several sets of constants A_s , A_p , Q' will produce the *same* energy level scheme, many sets of transition frequencies appear twice in the table (e.g., the first two lines).

The values of A_s , A_p , and Q' tabulated in Table II were obtained using a FORTRAN program with the University of Illinois IBM 7094 computer. There are really twice as many solutions as are shown, since the sign of Q' can be changed by reversing the order of the energy levels E_1 through E_4 , or the frequencies ν_1 and ν_3 ; these extra solutions are redundant since we have no method for determining the sign of Q' from the ENDOR frequencies.

If the spin Hamiltonians written down in Eqs. (2), (3), and (4) are correct, only one set of constants A_s , A_p , and Q' are necessary to completely determine the ENDOR spectrum for a given chlorine isotope. But, Table II shows that the best agreement obtainable between sets of constants calculated from the $M_s = +\frac{3}{2}$ and $M_s = -\frac{3}{2}$ spectrum is to within 100 to 200 kc/sec. The disagreement obtained between constants therefore

TABLE II. Possible Cl^{35} hyperfine and quadrupole constants from the $M_s = +\frac{3}{2}$ and $-\frac{3}{2}$ ENDOR frequencies.

ENDOR transitions				$(M_s = +\frac{3}{2} \text{ spectrum})$			$(M_s = -\frac{3}{2} \text{ spectrum})$		
ν_x	ν_y	ν_z		A_s (Mc/sec)	A_p (Mc/sec)	Q' (Mc/sec)	A_s (Mc/sec)	A_p (Mc/sec)	Q' (Mc/sec)
ν_1	ν_2	ν_3	(I)	8.364	1.513	5.650	8.430	1.625	5.830
ν_1	ν_2	ν_3		6.128	1.124	10.818	5.353	1.071	13.265
ν_1	ν_2	ν_5		7.274	0.395	-3.205	5.789	2.879	-1.527
ν_1	ν_2	ν_5		5.216	0.222	-8.504	3.286	0.718	-11.025
ν_1	ν_3	ν_2		4.493	0.486	-13.977	3.897	0.396	-16.179
ν_1	ν_3	ν_4		6.434	0.822	-3.160	5.318	0.527	-5.433
ν_1	ν_3	ν_4		4.576	0.508	-7.750	4.213	0.439	-8.408
ν_1	ν_3	ν_5			no solution		6.396	0.703	-3.913
ν_1	ν_3	ν_5		4.529	0.497	-9.549	4.037	0.416	-9.862
ν_1	ν_5	ν_4			no solution		3.660	2.113	-3.404
ν_2	ν_1	ν_3	(II)	4.868	1.656	12.354	4.363	1.481	14.588
ν_2	ν_1	ν_3		8.117	3.080	3.626	8.206	3.186	3.786
ν_2	ν_1	ν_5		3.814	0.212	-9.549	2.174	0.729	-11.363
ν_4	ν_1	ν_3		5.765	1.812	6.237		no solution	
ν_4	ν_1	ν_3		4.885	1.704	7.922		no solution	
ν_4	ν_1	ν_5		5.419	1.244	5.578		no solution	
ν_4	ν_1	ν_5		4.880	1.167	6.704		no solution	
ν_4	ν_1	ν_6			no solution		2.653	0.833	-4.346
ν_4	ν_1	ν_6			no solution		2.347	0.790	-4.999
ν_4	ν_2	ν_3		5.625	3.144	4.636	4.073	4.248	4.649
ν_4	ν_2	ν_6		2.437	0.608	6.712		no solution	
ν_4	ν_3	ν_5			no solution		1.394	1.109	8.670
ν_4	ν_5	ν_6			no solution		3.261	0.570	-2.988
ν_4	ν_5	ν_6			no solution		2.124	0.422	-5.684

far exceeds the experimental error in measuring the ENDOR frequency peak positions (the error ranges from ± 10 kc/sec to ± 40 kc/sec). In fact, there are two sets of constants, denoted in Table II by (I) and (II), which show the same order of agreement.

We may take the average values of the set (I) or set (II) constants obtained from the $M_s = +\frac{3}{2}$ and $M_s = -\frac{3}{2}$ ENDOR data and then calculate the observed Cl^{35} ENDOR frequencies for the entire spectrum. Likewise, using Cl^{37} constants derived from the Cl^{35}

constants by multiplying A_s and A_p by the nuclear-magnetic-moment ratio and Q' by the quadrupole-moment ratio, we can calculate the observed Cl^{37} ENDOR frequencies. The comparison between the calculated and the observed ENDOR frequencies is shown in Table III.

From Table III, we conclude that set (I) is the correct set of averaged spin Hamiltonian constants rather than set (II), because they predict the positions of the $M_s = -\frac{1}{2}$ and the $M_s = -\frac{5}{2}$ experimental ENDOR frequencies more accurately.

TABLE III. Comparison of calculated ENDOR frequencies with ENDOR data using the two "best" sets of spin-Hamiltonian constants.

(a) Average Values of Constants (in Mc/sec)					
Isotope	Set (I)		Set (II)		
	Cl^{35}	Cl^{37}	Cl^{35}	Cl^{37}	
A_s	8.40	6.99	8.16	6.79	
A_p	1.57	1.31	3.13	2.61	
Q'	5.74	4.52	3.71	2.92	
(b) Experimental and calculated ENDOR frequencies (Mc/sec)					
M_s	H_0 (G)	Isotope	Experimental	From set (I)	From set (II)
$+\frac{3}{2}$	3366.9	Cl^{35}	18.69 \pm 0.02	19.008	18.970
			11.66 \pm 0.02	11.669	11.739
			8.435 \pm 0.01	8.435	8.427
$-\frac{1}{2}$	3329.3	Cl^{37}	7.20 \pm 0.015	7.259	7.113
			7.90 \pm 0.01	8.153	9.154
			6.47 \pm 0.01	6.666	7.583
$-\frac{3}{2}$	2968.3	Cl^{35}	20.89 \pm 0.04	20.601	20.618
			14.13 \pm 0.03	14.119	14.037
			11.49 \pm 0.02	11.500	11.486
$-\frac{5}{2}$	3329.3	Cl^{37}	9.705 \pm 0.01	9.779	9.640
			21.42 \pm 0.03	21.333	23.867
		Cl^{35}	20.52 \pm 0.02	21.237	20.152
			17.86 \pm 0.05	17.805	19.901
			17.21 \pm 0.05	17.693	16.903

D. Quadrupole Constants for the Misaligned External Field

If we take the $M_s = +\frac{3}{2}$ ENDOR frequencies observed on the $M_s = +\frac{5}{2} \leftrightarrow +\frac{3}{2}$ transition as plotted in Fig. 4, we see that there are three sets of four ENDOR lines, with one line in each set for each chlorine ion of the tetrahedral site. We do not know *a priori* which three frequencies belong to one chlorine site, but we would expect that each set of three frequencies will yield the same quadrupole constant, Q' , assuming that the electric-field gradient is the same at each chlorine nucleus.

We look for values of Q' obtained using the same assignment of ENDOR transition frequencies, ν_1 , ν_2 , and ν_3 , as in set (I) in Table II. One choice of four sets of three frequencies yields values of Q' as given in Table IV. We see that the agreement of the calculated values of Q' is no better than within 300 kc/sec; other choices of four sets of three frequencies yield even more widely differing values of Q' .

VI. DISCUSSION AND CONCLUSIONS

A feature which distinguishes the present experiment from most ENDOR experiments is that the spin of the paramagnetic center studied here is $\frac{5}{2}$. Most of the reported ENDOR experiments deal with spin- $\frac{1}{2}$ centers which therefore do not include a crystal-field-splitting term in the complete spin Hamiltonian for the center. ENDOR of Cr^{3+} in Al_2O_3 ¹⁷ and of Fe^{3+} in silicon²¹ have been reported, but no effects of the crystal field on the ENDOR frequencies are discussed.

Recently, attention has been given to the effects of crystal fields on the hyperfine structure of Mn^{2+} in various host lattices including MgO ^{22,23} and SrCl_2 ²⁴ "Forbidden" transitions^{25,26} are observed, which are explained as due to the mixing of nuclear spin states by cubic or axial crystal fields. These transitions appear when the external field is not parallel to a crystal field axis, increasing as the angle between the field and the crystal field axis is increased.

Fry, Llewellyn, and Pryce²⁷ have pointed out mechanisms by which the cubic field splitting affects the ENDOR spectrum of Mn^{2+} , which is isoelectronic with Fe^{3+} . One effect is the mixing of electron-spin states, which alters the expectation value of S_z and, therefore, the magnitude of the effective magnetic field seen by the nucleus. Another effect of the cubic field is to tilt the direction of the effective magnetic field seen by the nucleus. This effect may be thought of as a "torque" produced on the axis of quantization of the electron spin by the cubic field, tending to pull this axis from the external field direction toward a cubic symmetry axis.

In our experiment with the external field making an angle of 0.5 deg with a $\langle 100 \rangle$ axis, we have minimized this "tilting effect" by bringing the external field nearly parallel to a $\langle 100 \rangle$ axis. The perturbing effect of the cubic field on the expectation value of S_z is also minimized; the term, $a(S_+^4 + S_-^4)/48$, is the only off-diagonal term in the cubic field, and this term produces a second-order correction to the expectation value of S_z . This correction is of order $(a/g\beta H_0)^2$ which is about 10^{-3} and leads to discrepancies in the hyperfine constants in the order of 10 kc/sec, which is too small to explain the 100 to 200 kc/sec differences between the hyperfine constants calculated from the $M_s = +\frac{3}{2}$ and the $M_s = -\frac{3}{2}$ spectrum. Likewise, second-order hyperfine interaction corrections, of order 10 kc/sec do not explain these discrepancies.

²¹ H. H. Woodbury and G. W. Ludwig, Phys. Rev. **117**, 102 (1960).

²² J. E. Drumheller and R. S. Rubins, Phys. Rev. **133**, A1099 (1964).

²³ G. J. Wolga and R. Tseng, Phys. Rev. **133**, A1563 (1964).

²⁴ G. L. Bir and L. S. Sochava, Fiz. Tverd. Tela **5**, 3594 (1963) [Engl. transl.: Soviet Phys.—Solid State **5**, 2637 (1964)].

²⁵ B. Bleaney and R. S. Rubins, Proc. Phys. Soc. **77**, 103 (1961).

²⁶ G. L. Bir, Fiz. Tverd. Tela **5**, 2236 (1963) [Engl. transl.: Soviet Phys.—Solid State **5**, 1628 (1964)].

²⁷ P. J. I. Fry, P. M. Llewellyn, and M. H. L. Pryce, Proc. Roy. Soc. **266**, 84 (1962).

TABLE IV. Calculated Cl^{35} quadrupole constants for the four chlorine sites with H_0 10 deg from $A \langle 100 \rangle$ axis.

ENDOR frequencies (in Mc/sec)			Calculated Q' (Mc/sec)
ν_1	ν_2	ν_3	Q'
13.033 ± 0.005	9.338 ± 0.003	18.030 ± 0.015	5.636 ± 0.025
12.682 ± 0.005	8.916 ± 0.005	18.350 ± 0.020	5.753 ± 0.030
10.900 ± 0.010	8.865 ± 0.003	19.430 ± 0.010	5.477 ± 0.025
10.387 ± 0.005	8.644 ± 0.005	19.745 ± 0.010	5.525 ± 0.020

Thus, the spin Hamiltonians expressed in Eqs. (1), (2), and (3) do not appear to be able to explain (1) the discrepancies between the $M_s = +\frac{3}{2}$ and $M_s = -\frac{3}{2}$ spin-Hamiltonian constants A_s , A_p , and Q' , or (2) the result that the quadrupole constants Q' for the four sites differ from one another by as much as 300 kc/sec when the external field is about 10 deg from a $\langle 100 \rangle$ axis.

To remove these discrepancies, it may be necessary to regard the spin-Hamiltonian "constants" as functions of M_s and of the orientation angles made by the external field with the nuclear quadrupole axes (the $[111]$ directions). Going a step further, if the quadrupole constants Q' are functions of M_s and the orientation of the external field, the spatial part of the electronic ground-state wave function for the iron-chlorine complex must also be a function of these quantities. This follows because the electric field gradients (which determine Q') at the four sites are determined by the spatial part of the electronic wavefunction evaluated at the chlorine nuclear sites.

No ENDOR lines attributable to silver nuclei were identified in the frequency range between 6 to 24 Mc/sec. Very few ENDOR lines were seen in the range of 3 to 6 Mc/sec on any of the five electron-spin-resonance transitions. About 50 closely spaced ENDOR lines were seen on the $M_s = +\frac{1}{2} \leftrightarrow -\frac{1}{2}$ transition in the range from 900 kc/sec to 3 Mc/sec, and a similar number of lines were seen on the other four transitions. Lines identified as "distant ENDOR"¹² lines for both Cl^{35} and Cl^{37} isotopes were seen with large signal-to-noise ratio in this frequency range.

It is these low-frequency ENDOR lines, due to more distant neighbor nuclei to the iron, which furnish a possible means for distinguishing between the three tetrahedral site models described in the Introduction. Analysis of these lines is made difficult by the complexity of the spectrum and the numerous lines observed in a small frequency range. Studies of these low-frequency ENDOR lines are now in progress.

The quadrupole frequency ν_Q related to Q' by the relationship $\nu_Q = 2Q'$ is equal to 11.48 Mc/sec and lies in the range of quadrupole resonance frequencies reported for typical iron-group chloride compounds by Barnes, Segel, and Jones.²⁸ These quadrupole frequencies range from 4.17 Mc/sec for TiCl_2 to 12.85 Mc/sec for

²⁸ R. G. Barnes, S. L. Segel, and W. H. Jones, J. Appl. Phys. **33**, 2965S (1962).

TABLE V. Hyperfine and quadrupole constants for Cl^{35} (in units of 10^{-4} cm^{-1}).

	ENDOR	ESR
$A = A_s + 2A_p$	3.85 ± 0.06	3.3 ± 0.5
$B = A_s - A_p$	2.28 ± 0.04	2.0 ± 0.5
$P' = Q'$	1.91 ± 0.04	1.0 ± 0.5

CrCl_3 . Narath²⁹ reports a value of the quadrupole frequency for Cl^{35} in anhydrous FeCl_3 of 10.118 Mc/sec. The fact that our value of ν_Q is comparable to these values for covalent iron-group chloride compounds suggests that the Fe^{3+} ion has an appreciable covalent bonding with its chlorine nearest neighbors and corroborates the suggestion by Hayes, Pilbrow, and Slifkin² that this defect may be regarded as a molecular-ion complex.

Table V shows the comparison of the spin-Hamiltonian constants obtained from the [100] ENDOR spectrum with those obtained by Hayes, Pilbrow, and Slifkin from fitting the lines shape of the electron-spin-resonance superhyperfine structure. The uncertainties given for the values of the constants obtained from the ENDOR spectrum are equal to the differences between the constants obtained from the $M_s = +\frac{3}{2}$ and the $M_s = -\frac{3}{2}$ Cl^{35} spectra plus the additional uncertainty of the ENDOR frequency measurements (which is about $0.01 \times 10^{-4} \text{ cm}^{-1}$).

The agreement between the two sets of hyperfine constants is within the experimental uncertainty, but the quadrupole constant obtained from the ENDOR data is nearly twice as large as that obtained from the electron-spin-resonance data. (This discrepancy may be due to the approximations required to fit the electron-spin-resonance line shape.) The agreement between the values of the hyperfine constants obtained from the two experiments confirms that (1) the correct spin-Hamiltonian constants were chosen from the many possibilities listed in Table II and, (2) the superhyperfine structure of the central electron-spin-resonance line are due to the four nearest neighbor, tetrahedrally coordinated, chlorine ions.

In summary, we have shown from the angular dependence of the ENDOR spectrum that the cubic spectrum of Fe^{3+} in silver chloride is due to iron in a tetrahedral site surrounded by four nearest-neighbor chlorine ions aligned along [111] directions from the iron. In addition, we have obtained hyperfine and quadrupole constants which explain to an accuracy of several hundred kilocycles per second the complete ENDOR spectrum from 6 to 24 Mc/sec with the external field applied along a (100) axis of the crystal. The discrepancies between the spin-Hamiltonian constants derived from the $M_s = +\frac{3}{2}$ and $M_s = -\frac{3}{2}$ spectra are not understood, but they do not appear to arise from effects of the cubic field-splitting term in the electron spin Hamiltonian.

²⁹ A. Narath, J. Chem. Phys. 40, 1169 (1964).

ACKNOWLEDGMENTS

The author would like to express his gratitude to Professor C. P. Slichter under whose supervision this work was performed. The silver chloride crystals used in this investigation were obtained from Professor F. C. Brown and Kodak Research Laboratories. Special thanks are given to Joe H. Pifer for his assistance in taking the ENDOR data. The author would also like to thank Elmer E. Lewis for his help in programming for the IBM 7094 Computer.

APPENDIX I: IDENTIFICATION OF NUCLEAR SPECIES BY "FIELD SHIFTS"

In this Appendix, we discuss the method by which the ENDOR lines between 6 and 24 Mc/sec were proved to be due to chlorine rather than silver nuclei.

Equation (10) in Appendix II gives the relationship of the effective Larmor frequency ν_0 in an effective field H_{eff} to the hyperfine constants, the M_s value, the nuclear frequency ν_n in the external field alone, and the angle between the external field and axis of symmetry of the hyperfine interactions. This formula is, in fact, the expression for the ENDOR frequency for a $\Delta M_I = \pm 1$ transition if the quadrupole interaction constant is zero.¹⁸

The ENDOR lines shown in Figs. 3 and 4 are such that lines of negative M_s shift upward in frequency as the external field H_0 is increased from one ESR transition to the other, while the lines with positive M_s (only $M_s = +\frac{3}{2}$ lines were identified) shift downward in frequency with increasing magnetic field. This behavior is exactly that predicted from Eq. (10) assuming A_s and A_p are positive, so we now may ask: How can this "field-shift" information be used to identify whether the lines are due to silver or to chlorine nuclei?

Both isotopes of silver have spin $\frac{1}{2}$ and therefore no quadrupole interaction. Therefore, the "field shift," $\Delta\nu_0$ can never be greater than $\Delta\nu_n$ for silver nuclei, where $\Delta\nu_n$ is the change in the nuclear frequency ν_n due to the change of external field. This is equivalent to saying that the change of the magnitude of the effective field is always less than or equal to the change of the external field. The shift $\Delta\nu_0$ is equal to $\Delta\nu_n$ if and only if $A_p = 0$.

Typical measured field shifts for ENDOR lines are given in Table VI.

Comparison of the observed ENDOR frequency shifts with the calculated values of $\Delta\nu_n$ for the chlorine and silver isotopes shows that the frequency shifts are greater than either value of $\Delta\nu_n$ for silver, and consequently the ENDOR lines cannot be due to silver and can only be due to chlorine.

The reason that some of the observed "field shifts" are larger than $\Delta\nu_n$ for Cl^{35} is that the quadrupole interaction contribution to the ENDOR frequencies is quite large. When the external field is changed, the

TABLE VI. "Field shifts" for $M_s = +\frac{3}{2}$ ENDOR lines for H_0 10 deg from A [100] direction. (ENDOR frequencies are given for the $M_s = +\frac{3}{2} \leftrightarrow +\frac{1}{2}$ transition.)

ENDOR frequency (Mc/sec)	ENDOR frequency shift (Mc/sec)	ENDOR frequency (Mc/sec)	ENDOR frequency shift (Mc/sec)
19.745	0.209±0.030	10.900	0.107±0.014
19.430	0.242±0.030	10.387	0.116±0.009
18.350	...	9.338	0.147±0.007
18.030	0.310±0.030	8.916	0.161±0.009
13.033	0.143±0.010	8.865	0.151±0.006
12.682	0.124±0.011	8.644	0.152±0.008
$\Delta\nu_n(\text{Cl}^{35}) = 0.132$ Mc/sec		$\Delta\nu_n(\text{Ag}^{107}) = 0.055$ Mc/sec	
$\Delta\nu_n(\text{Cl}^{37}) = 0.110$ Mc/sec		$\Delta\nu_n(\text{Ag}^{109}) = 0.063$ Mc/sec	

direction of the effective field is changed with respect to the quadrupole-interaction axis (since $A_p \neq 0$). This causes the nuclear spin to "tilt" with respect to the electric-field gradients and changes the magnitude of the quadrupole energy of the nucleus.

APPENDIX II. CALCULATION OF THE HYPERFINE AND QUADRUPOLE CONSTANTS FROM THE ENDOR FREQUENCIES

Suppose we are given three experimental ENDOR frequencies (which we assume to be positive quantities) out of the six possible ENDOR frequencies (see Fig. 7). If we assume that these frequencies belong to three specified transitions between energy levels, we can calculate the energy levels and the other three frequencies. If any of these calculated frequencies turn out to be negative, we know that the original assumption is incorrect, for we require that all six frequencies be related by an energy level scheme as shown in Fig. 7.

Having either assumed or calculated the values of ν_1 , ν_2 , and ν_3 and, using the sum rules for the energy levels of a spin- $\frac{3}{2}$ nucleus with both a Zeeman and quadrupole interaction,²⁰ we can write the following equations and evaluate A , B , and C :

$$A \equiv 5\nu_0^2 + \nu_Q^2 = (\nu_1^2 + \nu_3^2)/2 + \nu_x^2, \quad (6)$$

$$B \equiv 4\nu_Q\nu_0^2(3 \cos^2\eta - 1) = \nu_x(\nu_3^2 - \nu_1^2), \quad (7)$$

$$C \equiv \nu_Q^4 + 9\nu_0^4 + 2\nu_0^2\nu_Q^2(1 - 6 \cos^2\eta), \quad (8)$$

$$= (\nu_x^2 - \nu_1^2)(\nu_x^2 - \nu_3^2),$$

where we define the following quantities:

$$\nu_x \equiv \nu_2 + (\nu_1 + \nu_3)/2,$$

$$\nu_Q \equiv 2Q',$$

$$\nu_0 \equiv |\gamma_n \hbar \mathbf{H}_{\text{eff}}|,$$

and η is the angle between the quadrupole axis and the effective magnetic field direction.

To solve the equations for ν_Q , ν_0 , and η , we first obtain solutions for the quadrupole frequency ν_Q from the fourth-order polynomial equation

$$44\nu_Q^4 - 28A\nu_Q^2 - 25B\nu_Q + 9A^2 - 25C = 0. \quad (9)$$

We discard any of the four roots whose imaginary part is, say, greater than 1 kc/sec. We substitute each of the real roots, positive or negative, into (6) to find ν_0 , and into (7) to find η .

The effective Larmor frequency ν_0 in the effective field H_{eff} is related to the hyperfine constants, A_s and A_p , by

$$\nu_0 = \{[A_s M_s - \nu_n + A_p M_s(3 \cos^2\theta - 1)]^2 + (3A_p M_s \sin\theta \cos\theta)^2\}^{1/2}, \quad (10)$$

where θ is the angle between the external field and the quadrupole axis, and ν_n is the nuclear resonance frequency $\gamma_n \hbar H_0$ of the chlorine nucleus in the external field.

The angle η and the angle θ are related by

$$\cos\eta = \cos(\theta - \phi), \quad (11)$$

where ϕ is defined by

$$\tan\phi \equiv \frac{3A_p M_s \sin\theta \cos\theta}{M_s(A_s - A_p + 3A_p \cos^2\theta) - M_s \nu_n / |M_s|}. \quad (12)$$

We cannot determine the hyperfine constants, A_s and A_p , from ν_0 and η unless θ is known. We know $\theta = 54.73561$ deg when the external field is parallel to a [100] direction, because it makes this angle with each of the $\langle 111 \rangle$ axes. In this case ($\cos^2\theta = \frac{1}{3}$), we may find the hyperfine constants from

$$A_s = \nu_0(\sqrt{2} \cos\eta + 2 \sin\eta)/6^{1/2} |M_s| + \nu_n/M_s \quad (13)$$

and

$$A_p = \nu_0(\sqrt{2} \cos\eta - \sin\eta)/6^{1/2} |M_s|. \quad (14)$$